

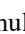


# An Event-Driven Closed-Loop Ultrasound Stimulator Composed of a Micro-Transducer and Multi-Site Electrodes in Vitro

Ryo Furukawa<sup>1</sup>, Shuichi Murakami<sup>2</sup> and Takashi Tateno<sup>3</sup>

<sup>1</sup>Bioengineering and Bioinformatics, Graduate School of Information Science and Technology, Hokkaido University, Kita 14, Nishi 9, Kita-ku, Sapporo, Hokkaido 060-0814, Japan

<sup>2</sup>Osaka Research Institute of Industrial Science and Technology, 2-7-1, Ayumino, Izumi, Osaka, 594-1157, Japan

<sup>3</sup>Bioengineering and Bioinformatics, Faculty of Information Science and Technology, Hokkaido University, Kita 14, Nishi 9, Kita-ku, Sapporo, Hokkaido 060-0814, Japan

**Keywords:** Brain Slice, Calcium Imaging, Closed-Loop System, Micromachined Transducer, Ultrasound Stimulation.

**Abstract:** Ultrasound neuromodulation, in which local and deep brain areas are stimulated, holds promise for clinical applications. However, the mechanisms of action underlying the stimulation effects are still unknown. In vitro experiments are helpful for investigating the stimulation mechanisms because they allow easy control of extracellular conditions. Compared with closed-loop systems, conventional open-loop systems do not permit monitoring of neural activity, and thus can lead to excessive neural stimulation. In this study, we developed a piezoelectric micromachined ultrasound transducer (PMUT) combined with monitoring microelectrodes. To examine the potential of our device as a neuromodulation tool, we measured the cellular responses to generated ultrasound stimulation. Subsequently, we constructed a closed-loop system that combined our PMUT with monitoring electrodes, and applied event-related ultrasound stimulation to brain slices in vitro. We discuss future applications of a closed-loop ultrasound stimulation system.


## 1 INTRODUCTION


Ultrasound stimulation enables non-invasive stimulation of local and deep areas of the brain, which are difficult to achieve using conventional electromagnetic stimulation methods (Tufail et al., 2010; Wagner et al., 2007). However, the cellular mechanisms of ultrasound-induced neural activation are unclear. Furthermore, little is known about how cellular responses to ultrasound stimulation influence localized neural networks in vivo. For example, indirect neural activity in the auditory pathway could affect neuromodulation, complicating investigations of the mechanism of action (Sato et al., 2018).


Most current brain stimulation strategies are limited in terms of their ability to control patterns of brain activity. This is because they generally involve unidirectional stimulation processes, and thus do not capture sufficient information about the neural activity surrounding the stimulator. Flexible

regulation of neural activity could be achieved via closed-loop approaches to brain stimulation, including ultrasound stimulation. Accordingly, researchers have prioritized the creation of microelectrodes and small-scale stimulators within the same device, along with the development of bidirectional technological approaches that enable simultaneous stimulation and recording of neural activity.

When examining the cellular mechanisms underlying the effects of ultrasonic stimulation, in vitro experimental systems enable easy control of the extracellular conditions around neurons. Lee et al. developed a piezoelectric micromachined ultrasound transducer (PMUT) that was helpful in elucidating the cellular mechanisms of neuromodulation in dissociated cultured neurons in vitro (Lee et al., 2019). However, in their experiments, which used dissociated cultured cells, the original neural networks were rebuilt in networks with random

 <https://orcid.org/0000-0001-8920-1025>

 <https://orcid.org/0000-0002-8862-8446>

 <https://orcid.org/0000-0001-9429-9880>

connections. Furthermore, conventional open-loop stimulators can induce excessive neural activity, something which could be addressed by closed-loop stimulation (Takeuchi & Berényi, 2020). Several reports have described methods for closed-loop ultrasound stimulation (Jo et al., 2022; Xie et al., 2022). However, in these studies, the stimulator and monitoring electrodes were not packaged together as one instrument. Considering future applications for chronic conditions, systems using an integrated device are optimal.

In this study, we firstly describe the design and fabrication of a PMUT combined with monitoring microelectrodes. We used microelectromechanical systems (MEMS) technology for microfabrication. Next, we conducted intracellular calcium imaging in vitro to examine whether the device could be used for ultrasound neuromodulation. Finally, we constructed a closed-loop system including our PMUT and microelectrodes, and conducted event-related ultrasound stimulation.

## 2 METHODS

### 2.1 Design, Microfabrication, and Packaging

To locally stimulate a brain slice, we aimed to develop a PMUT that satisfied three numerical conditions: (i) a diaphragm resonant frequency of 500 kHz, (ii) a stimulation ultrasound pressure greater than 65 kPa, and (iii) a diaphragm radius smaller than 600  $\mu\text{m}$  (Lee et al., 2019; Oh et al., 2019).

Our PMUT consisted of the following five components: a piezoelectric film, a silicon (Si) layer, a SiO<sub>2</sub> membrane, top and bottom Pt/Ti electrodes, and a Si supporting layer (Fig. 1). To convert electric (voltage) signals into ultrasound pressures, we used a thin film of a piezoelectric material as the transducer.

Prior to microfabrication, we conducted a simulation using general-purpose physics simulation software (COMSOL Multiphysics, Ver. 5.5, COMSOL AB, Sweden) on a supercomputer system (PRIMERGY CX 400/CX2550, FUJITSU, Japan) at the Hokkaido University Computer Center. We calculated the resonant frequency (500 kHz) and determined the potential size range of the PMUT.

For microfabrication, the sizes of the circular diaphragms were set according to the simulation results. We created eight microelectrodes (200  $\times$  200  $\mu\text{m}^2$ ), patterned to monitor the neural activity of a brain slice (Fig. 1A). The fabricated PMUT was packaged with the printed circuit board (Fig. 1B,C).

### 2.2 Physical Properties

To characterize the resonant frequency of each diaphragm, we applied a sinusoidal voltage input from a multifunction generator (WF1947, NF Co., Japan) and measured the acoustic pressure using a needle hydrophone (HY05N, Toray Engineering Co., Japan). Subsequently, we assessed the electrical characteristics of the microelectrodes via electrochemical impedance spectroscopy. To characterize the electrochemical properties of the microelectrodes on the PMUT device, we used a potentiostat (Electrochemical Analyzer ALS720E, BAS Inc., Japan) with a built-in frequency analyzer (Takahashi et al., 2019).

### 2.3 Preparation of Brain Slices

All animal experiments described below were approved by the Institutional Animal Care and Use Committee of Hokkaido University and carried out in accordance with the National Institutes of Health Guidelines for the Care and Use of Laboratory Animals. Here, we used four C57BL/6J mice (two male and two female mice, 7–10 weeks old, Japan SLC Inc., Hamamatsu, Japan). Each mouse was deeply anesthetized with isoflurane and decapitated. The brains were rapidly removed and transferred into ice-cold artificial cerebral spinal fluid (119 NaCl, 2.5 KCl, 2.5 CaCl<sub>2</sub>, 1.3 MgSO<sub>4</sub>, 1.0 NaH<sub>2</sub>PO<sub>4</sub>, and 11.0 D-glucose, in mM, pH = 7.4). We prepared 400- $\mu\text{m}$  brain slices including the auditory cortex (Furukawa et al., 2022).

### 2.4 Calcium Imaging

Before attempting closed-loop ultrasound stimulation, we examined whether our PMUT could activate cells in a brain slice. To observe cellular activities, we used Fura-2 AM dye to image changes in the fluorescence of intracellular Ca<sup>2+</sup> concentrations. This enabled us to avoid ultrasound vibration artifacts (Qiu et al., 2019). Fura-2 AM is excitable at light wavelengths of either 340 or 380 nm and emits fluorescence at 510 nm. We alternately measured fluorescence intensities with excitation at 340 ( $F_{340}$ ) or 380 nm ( $F_{380}$ ) at a frame rate of 50 Hz (Tateno, 2010). Then, we estimated the ratiometric fluorescence intensity by calculating the  $F_{340}/F_{380}$  ratio. In the absence of stimulation, we first monitored baseline changes in Ca<sup>2+</sup> transients for a period of 1 s. Subsequently, we applied ultrasound stimulation (880 kHz, continuous wave,  $65.6 \pm 1.8$  kPa) for 1 s and imaged the Ca<sup>2+</sup> transients, followed by monitoring of the Ca<sup>2+</sup> transients during the recovery period for 1 s.

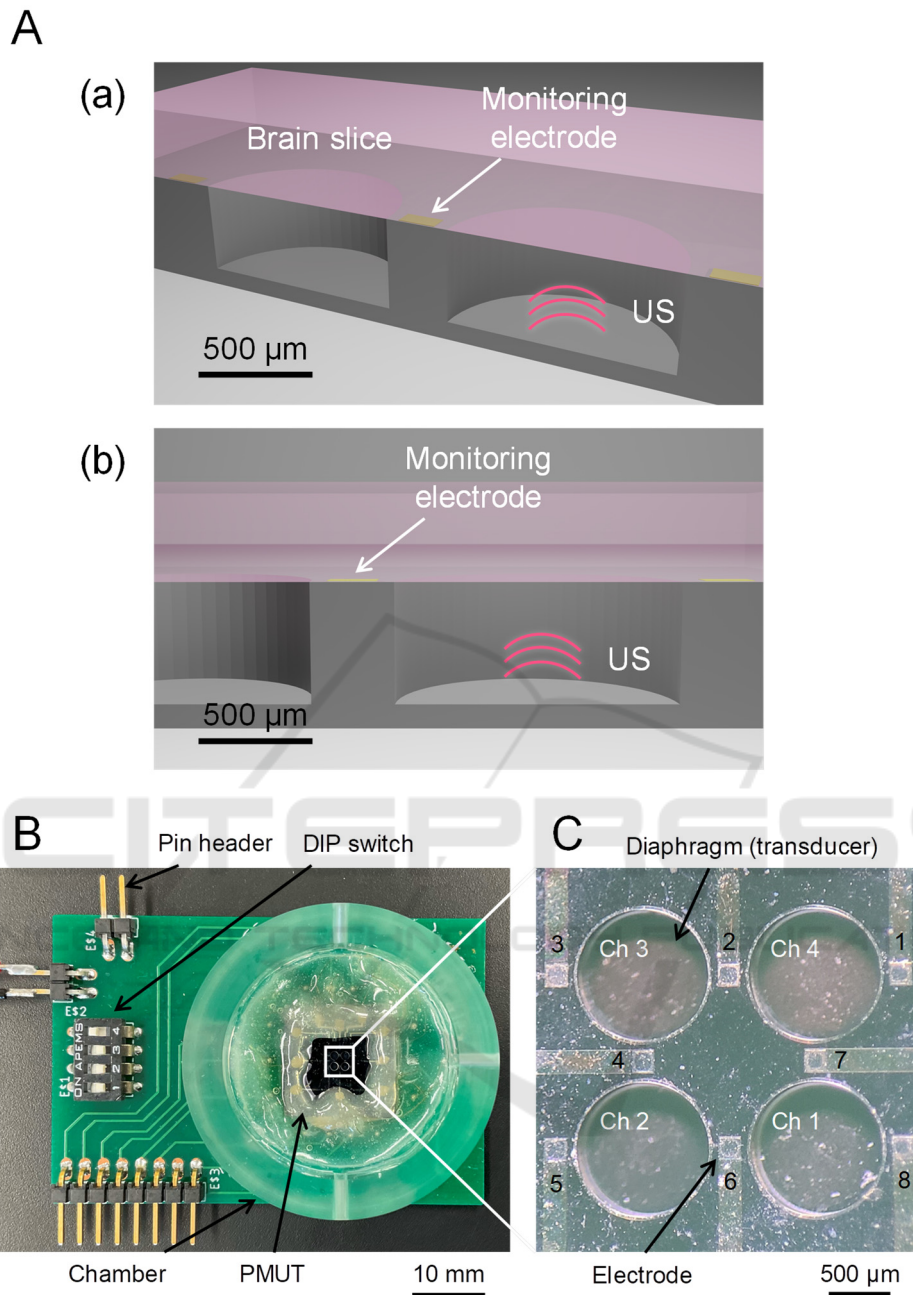


Figure 1: Structure and design of a PMUT device. (A) Schematic of the PMUT device under a brain slice. (a) Cross view. (b) Front side of the cross section. (B) A packaged substrate combined with the PMUT device. (C) The front side of the PMUT device with four diaphragms (four channels, chs. 1 to 4) and eight electrodes (1 to 8).

## 2.5 A Closed-Loop System Using Ultrasound Stimulation

Figure 2A illustrates a conventional open-loop ultrasound stimulation system, which evoked local field potential (LFP) responses (Fig. 2C, left) (Furukawa et al., 2022). Here, we examined a closed-loop system with a feedback pathway from the

packaged PMUT (Fig. 2B). In the closed-loop system, spontaneous brain slice activity was monitored while ultrasound stimulation was applied at the time point(s) when the activity exceeded a set threshold (Fig. 2C, right). We set the threshold at 150 μV. To monitor LFPs, we used a MED amplifier (MED-A64HS1, MED-A64MD1A, Alpha MED Scientific, Japan) from a previous MEA-based

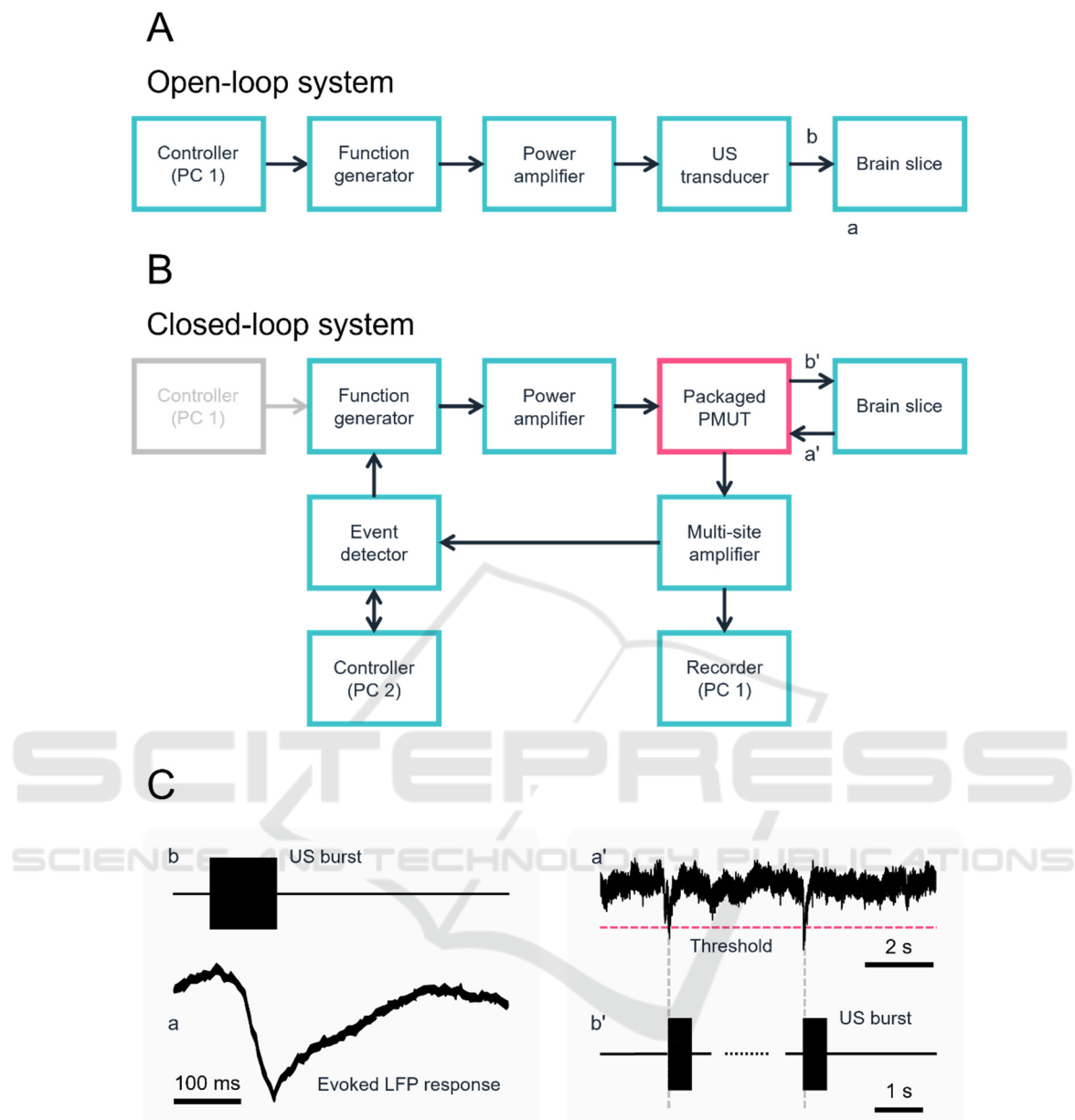


Figure 2: Schematic of ultrasound stimulation systems and related signals. (A) A block diagram of a conventional open-loop ultrasound stimulation system. (B) Our constructed closed-loop system with the packaged PMUT. (C) Schematic of activity detected via the extracellular voltage of a brain slice. The event detector sends trigger signals to the multifunction generator immediately after detecting LFP signals that negatively cross a threshold level. The left panel shows a typical evoked LFP response to ultrasound stimulation.

recording system (Furukawa et al., 2022). The signals were recorded with a sampling rate of 20 kHz, and subjected to filtering within a frequency range from 1 Hz to 10 kHz. We employed a multifunctional I/O data acquisition system (USB-6343, National Instruments, USA) for real-time signal control, which acquired neural signals from the MED amplifier and fed a trigger signal to a multifunction generator when

a threshold-crossing event was detected. We used a customized Python program (Python Ver. 3.11.1) for real-time processing. To detect neural activities, we used electrode 7 for monitoring. We applied ultrasound stimulation (540 kHz, continuous wave,  $95.5 \pm 1.4$  kPa) from a diaphragm (ch 4, which was close to electrode 7). For a single trial, the measurement period was 1 min.

### 3 RESULTS

#### 3.1 Microfabricated PMUT

According to the result obtained from our numerical simulation, we determined the optimal thickness of the material layers (PZT, 100  $\mu\text{m}$ ; Si, 15  $\mu\text{m}$ ; SiO<sub>2</sub>, 1  $\mu\text{m}$ ) and the radius (580  $\mu\text{m}$ ). We estimated that the diaphragm would oscillate with a resonant frequency of 540 kHz.

Our acoustic pressure measurement indicated forced diaphragm oscillations driven by voltage signals with a wide range of frequencies including 540 kHz, at which the oscillating amplitude had a positive peak (Fig. 3A).

When we increased the amplitude of the input voltage signal at a fixed frequency of 540 kHz, the output acoustic pressure was monotonically increased (Fig. 3B). The measured electrode impedance on the PMUT device was  $23.4 \pm 3.7 \text{ k}\Omega$  at 1 kHz (eight electrodes). Thus, the fabricated low impedance micro-electrodes were able to monitor LFPs from brain slices.

#### 3.2 Calcium Imaging

We next examined the possibility that our PMUT could activate cells. Figure 3C shows an example of Ca<sup>2+</sup> imaging (indicator, Fura-2 AM), with the averaged waveforms of the fluorescence intensity ratio obtained via ratiometric imaging (19 cells from

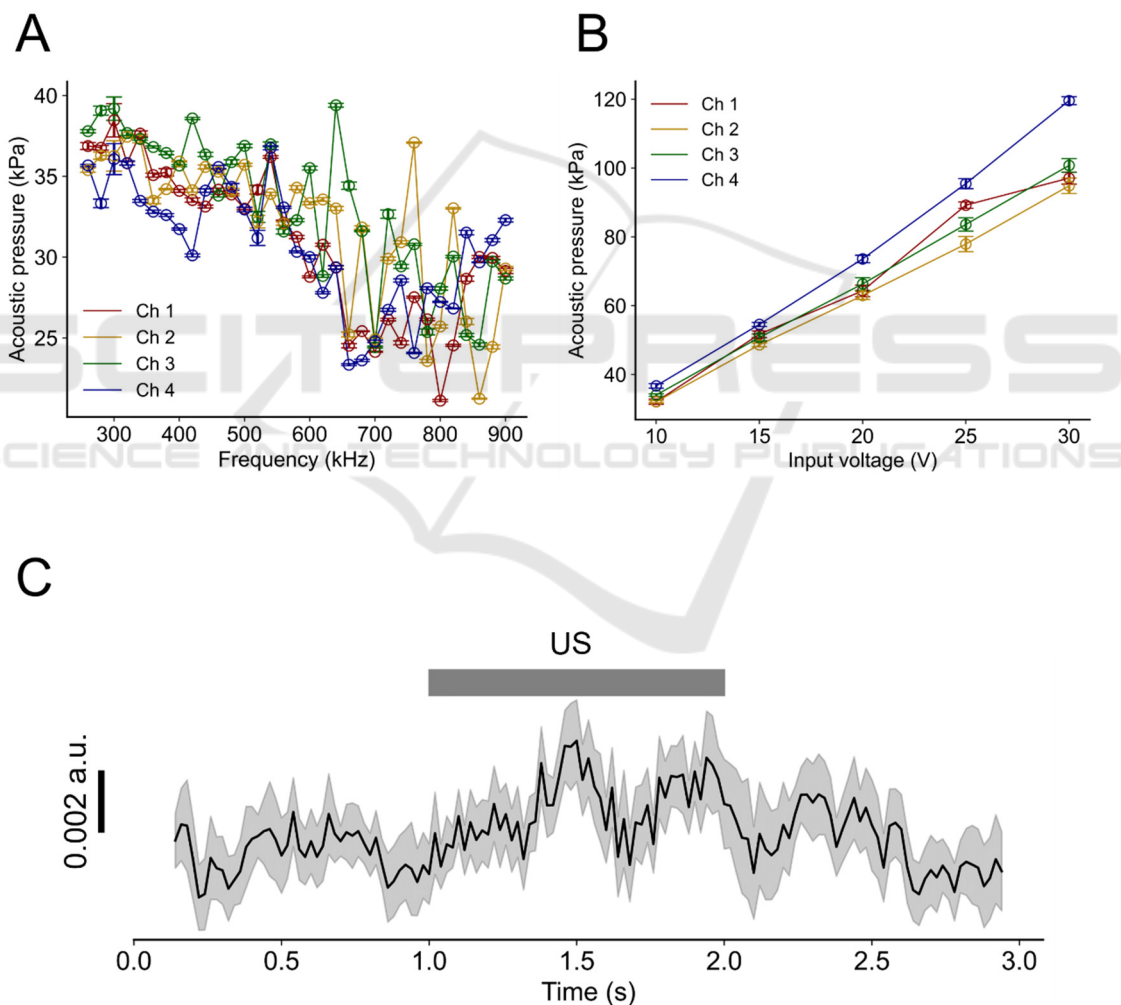


Figure 3: Measured acoustic characteristics of the fabricated PMUT and cellular activation via ultrasound stimulation. (A) Measured acoustic pressure vs. driving voltage signals with different sinusoidal frequencies (input voltage, 10 V). (B) Acoustic pressure with different input voltages under a fixed frequency of 540 kHz. The channel numbers correspond to those shown in Fig. 1D. (C) PMUT-driven average transients of ratiometric imaging (black) data related to intracellular Ca<sup>2+</sup> concentrations for all analysed cells. The edges of the grey band represent the standard error of the mean at each time point ( $n = 19$  cells from five slices). Grey bar indicates the duration of the ultrasound stimulation (US).



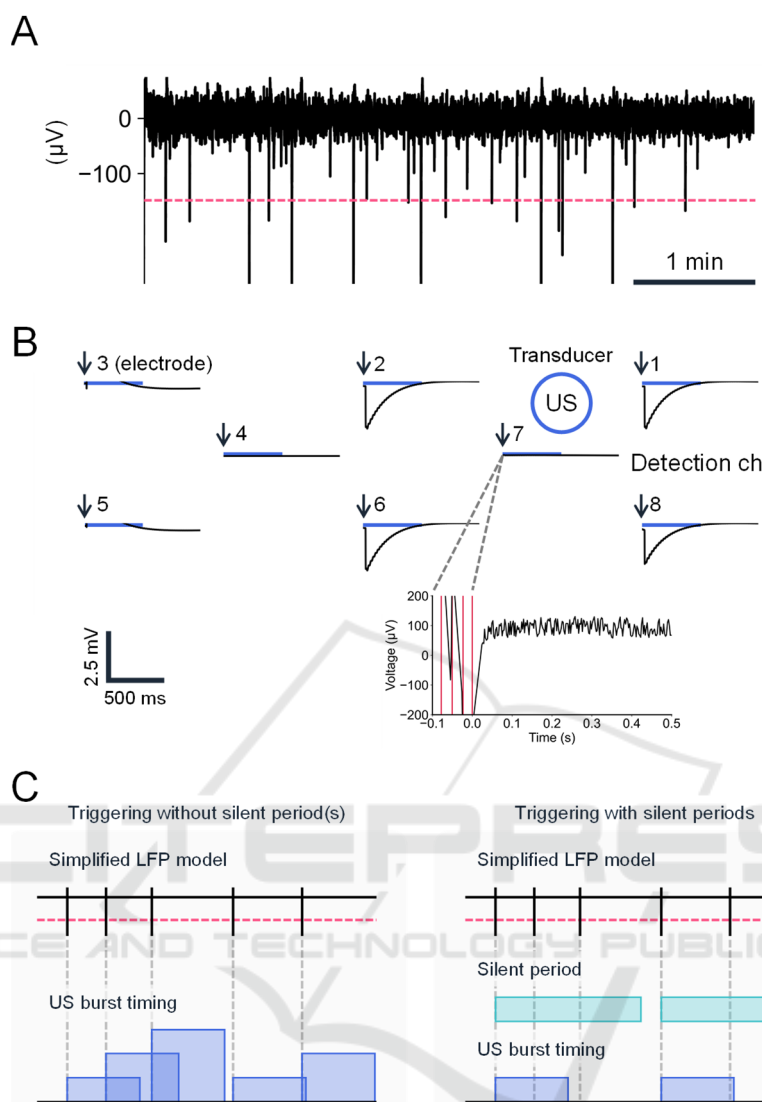


Figure 4: Closed-loop system with real-time detection of spontaneous activity in a brain slice. (A) A typical example of a spontaneous LFP waveform from a brain slice. The dashed red line indicates the threshold. (B) A typical example of spatiotemporal LFP recorded at eight microelectrode sites on the PMUT. The horizontal blue bars represent the timings of ultrasound stimulation (US; duration of each stimulation pulse, 500 ms). The blue circle represents the stimulation site; the schematic diagram shows only the relative positions of the recording electrodes and the stimulating diaphragms, and the actual distances between them differ. Electrode 7 was used for detection of spontaneous activity. In the bottom panel, the timings of threshold crossing are illustrated via vertical red lines. The time point of 0 ms is expressed with arrows in the top panel. (C) Schematic diagram of event detection and triggering methods. The current triggering method (left) had no refractory (silent) period(s), whereas our future triggering method will include this feature (right). Vertical bars represent event timings, and horizontal red lines indicate the threshold level for event detection. In the current system, the stimuli can overlap according to the timings of events occurring within 500 ms. In our future system, the silent period(s) will ensure that the US do not temporally overlap.

five slices). The intracellular  $Ca^{2+}$  concentration of the cells increased in response to ultrasound stimulation generated by the PMUT.

### 3.3 Event-Driven Ultrasound Stimulation

After confirming that our PMUT could modulate cellular activity, we next attempted to create a closed-loop system using ultrasound stimulation. A typical

example of LFP recording of a brain slice is illustrated in Fig. 4A. The negative peaks of rapid voltage changes in LFPs occurred randomly, and the peak events were detected as negative crossings below the threshold ( $-150 \mu\text{V}$ ). The inter-event intervals were  $15.5 \pm 1.1$  s for the seven channels for one brain slice.

When each event was detected (Fig. 4B), ultrasound stimulation was automatically applied to the brain slice from the PMUT. The stimulation was driven by an ultrasound signal generated by a functional generator through a power amplifier (Fig. 2B).

In our closed-loop system (Fig. 2B), peak-event detection was continuously functioning immediately after the onset of ultrasound stimulation and during each stimulus (500 ms). As a result, repetitive stimuli were triggered without a silent period (Fig. 4B). Therefore, a longer stimulation duration ( $> 500$  ms) could occur if the extracellular voltage continued to exceed the threshold level (Fig. 4C).

For example, Fig. 4B shows how the LFP responses rapidly decreased after the stimulation onset and slowly returned to individual baselines at four chs. (i.e., chs. 1, 2, 6, and 8), which were close to the ultrasound stimulation site (diaphragm ch. 4 in the transducer array). Since the LFP at the detection site (i.e., electrode ch. 7) exceeded the threshold voltage for a relatively longer period, trigger signals at multiple timings (four times in Fig. 4B, bottom) were sent to the multifunction generator, resulting in a stimulation duration over 500 ms (c.f., Fig. 4C, left).

## 4 DISCUSSION

In this study, we developed a MEMS-based PMUT with monitoring microelectrodes for event detection (i.e., rapid changes in LFP magnitude). We successfully microfabricated the PMUT with four circular diaphragms for ultrasound stimulation and eight microelectrodes for monitoring LFP-peak events. To demonstrate that our device could perform ultrasound neuromodulation, we conducted intracellular calcium imaging. An influx of  $\text{Ca}^{2+}$  into cells during ultrasound stimulation was successfully observed in acute brain slices. These intracellular  $\text{Ca}^{2+}$  transients suggest that our PMUT has potential for ultrasound neuromodulation applications.

Subsequently, we constructed a closed-loop system that included the PMUT as part of the ultrasound stimulator. To the best of our knowledge, this is the first attempt to combine a PMUT with electrodes that monitor cellular activity as an integrated device in a closed-loop system.

In our current system, ultrasound stimulation was automatically applied to the target when the detected signals were larger than the voltage threshold. Therefore, it was unclear whether the detected signals were truly attributable to spontaneous brain slice activity or were the result of electrical noise. We are planning to utilize more robust detection techniques to detect neural activity in our future work.

Upon improvements to the real-time detector in our system, our device could be applied to the detection of abnormal neural activity such as seizure-like activity (Berényi et al., 2012; Ranjandish & Schmid, 2020). In our next detector model, we are planning to include a silent period after each detected event as a triggering rule (Fig. 4C, right). This triggering rule could limit excessive stimulation. Moreover, we plan to test this device in in vivo animal experiments via chronic ultrasound stimulation.

## ACKNOWLEDGEMENTS

R.F. was supported by Grant-in-Aid for JSPS Fellows [grant number JP23KJ0047]. T.T. was supported by the Murata Science Foundation, the Suzuken Memorial Foundation, the Nakatani Foundation for Advancement of Measuring Technologies in Biomedical Engineering, a Grant-in-Aid for Exploratory Research [grant number 18K19794], and a Grant-in-Aid for Scientific Research (B) [grant number 19H04178] (Japan).

## REFERENCES

- Berényi, A., Belluscio, M., Mao, D., & Buzsáki, G. (2012). Closed-Loop Control of Epilepsy by Transcranial Electrical Stimulation. *Science*, 337(6095), 735–737. <https://doi.org/10.1126/science.1223154>
- Furukawa, R., Kaneta, H., & Tateno, T. (2022). A Multielectrode Array-Based Recording System for Analyzing Ultrasound-Driven Neural Responses in Brain Slices in vitro. *Frontiers in Neuroscience*, 16(February), 1–19. <https://doi.org/10.3389/fnins.2022.824142>
- Jo, Y., Lee, S. M., Jung, T., Park, G., Lee, C., Im, G. H., Lee, S., Park, J. S., Oh, C., Kook, G., Kim, H., Kim, S., Lee, B. C., Suh, G. S. B., Kim, S. G., Kim, J., & Lee, H. J. (2022). General-Purpose Ultrasound Neuromodulation System for Chronic, Closed-Loop Preclinical Studies in Freely Behaving Rodents. *Advanced Science*, 9(34). <https://doi.org/10.1002/ADVS.202202345>
- Lee, J., Ko, K., Shin, H., Oh, S.-J., Lee, C. J., Chou, N., Choi, N., Tack Oh, M., Chul Lee, B., Chan Jun, S., &

- Cho, I.-J. (2019). A MEMS ultrasound stimulation system for modulation of neural circuits with high spatial resolution in vitro. *Microsystems & Nanoengineering*, 5(1), Article 1. <https://doi.org/10.1038/s41378-019-0070-5>
- Oh, S. J., Lee, J. M., Kim, H. B., Lee, J., Han, S., Bae, J. Y., Hong, G. S., Koh, W., Kwon, J., Hwang, E. S., Woo, D. H., Youn, I., Cho, I. J., Bae, Y. C., Lee, S., Shim, J. W., Park, J. H., & Lee, C. J. (2019). Ultrasonic Neuromodulation via Astrocytic TRPA1. *Current Biology*, 29(20), 3386-3401.e8. <https://doi.org/10.1016/j.cub.2019.08.021>
- Qiu, Z., Guo, J., Kala, S., Zhu, J., Xian, Q., Qiu, W., Li, G., Zhu, T., Meng, L., Zhang, R., Chan, H. C., Zheng, H., & Sun, L. (2019). The Mechanosensitive Ion Channel Piezo1 Significantly Mediates In Vitro Ultrasonic Stimulation of Neurons. *iScience*, 21, 448–457. <https://doi.org/10.1016/j.isci.2019.10.037>
- Ranjandish, R., & Schmid, A. (2020). A Review of Microelectronic Systems and Circuit Techniques for Electrical Neural Recording Aimed at Closed-Loop Epilepsy Control. *Sensors*, 20(19), Article 19. <https://doi.org/10.3390/s20195716>
- Sato, T., Shapiro, M. G., & Tsao, D. Y. (2018). Ultrasonic Neuromodulation Causes Widespread Cortical Activation via an Indirect Auditory Mechanism. *Neuron*, 98(5), 1031-1041.e5. <https://doi.org/10.1016/j.neuron.2018.05.009>
- Takahashi, S., Muramatsu, S., Nishikawa, J., Satoh, K., Murakami, S., & Tateno, T. (2019). Laminar responses in the auditory cortex using a multielectrode array substrate for simultaneous stimulation and recording. *IEEJ Transactions on Electrical and Electronic Engineering*, 14(2), 303–311. <https://doi.org/10.1002/tee.22810>
- Takeuchi, Y., & Berényi, A. (2020). Oscillotherapeutics – Time-targeted interventions in epilepsy and beyond. *Neuroscience Research*, 152, 87–107. <https://doi.org/10.1016/j.neures.2020.01.002>
- Tateno, T. (2010). A small-conductance Ca<sup>2+</sup>-dependent K<sup>+</sup> current regulates dopamine neuron activity: A combined approach of dynamic current clamping and intracellular imaging of calcium signals. *NeuroReport*, 21(10), 667–674. <https://doi.org/10.1097/WNR.0b013e32833add56>
- Tufail, Y., Matyushov, A., Baldwin, N., Tauchmann, M. L., Georges, J., Yoshihiro, A., Tillery, S. I. H., & Tyler, W. J. (2010). Transcranial Pulsed Ultrasound Stimulates Intact Brain Circuits. *Neuron*, 66(5), 681–694. <https://doi.org/10.1016/j.neuron.2010.05.008>
- Wagner, T., Valero-Cabre, A., & Pascual-Leone, A. (2007). Noninvasive human brain stimulation. *Annual Review of Biomedical Engineering*, 9, 527–565. <https://doi.org/10.1146/annurev.bioeng.9.061206.133100>
- Xie, Z., Yan, J., Dong, S., Ji, H., & Yuan, Y. (2022). Phase-locked closed-loop ultrasound stimulation modulates theta and gamma rhythms in the mouse hippocampus. *Frontiers in Neuroscience*, 16(September), 1–12. <https://doi.org/10.3389/fnins.2022.994570>